

1 **Supplementary Data**

2 **Machine learning based classification of cells into chronological stages using single-cell**
3 **transcriptomics**

4 Sumeet Pal Singh, Sharan Janjuha, Samata Chaudhuri, Susanne Reinhardt, Annekathrin

5 Kränkel, Sevina Dietz, Anne Eugster, Halil Bilgin, Selçuk Korkmaz, John E. Reid, Gökmen

6 Zararsız, Nikolay Ninov

7

8 **Includes:**

9 Supplementary Figures S1 – S9

10 Supplementary Table S1-S5 Legends

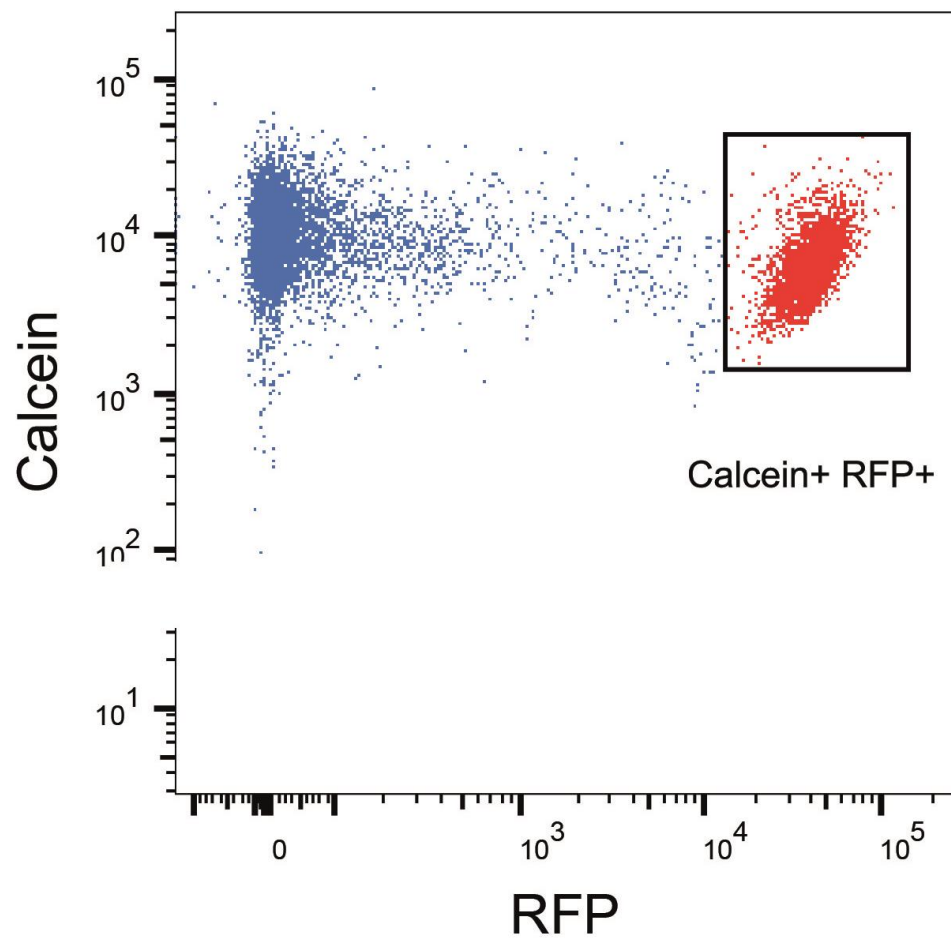
11 Supplementary Methods

12 Supplementary References

13

14 **Supplementary Figure S1**

15



16

17 **Supplementary Figure S1: FACS sort of zebrafish beta-cells**

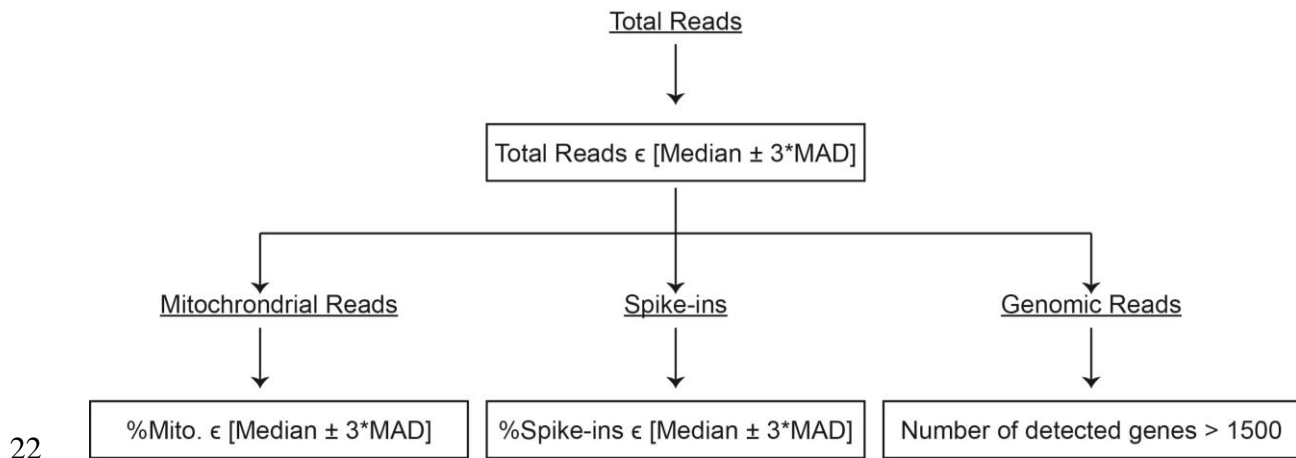
18 A FACS plot of live RFP-positive cells from *Tg(ins:BB1.0L)* animals at 3 mpf. Calcein labels

19 live cells, while RFP labels beta-cells.

20

21 **Supplementary Figure S2**

Quality Control for Single-cell Sequencing



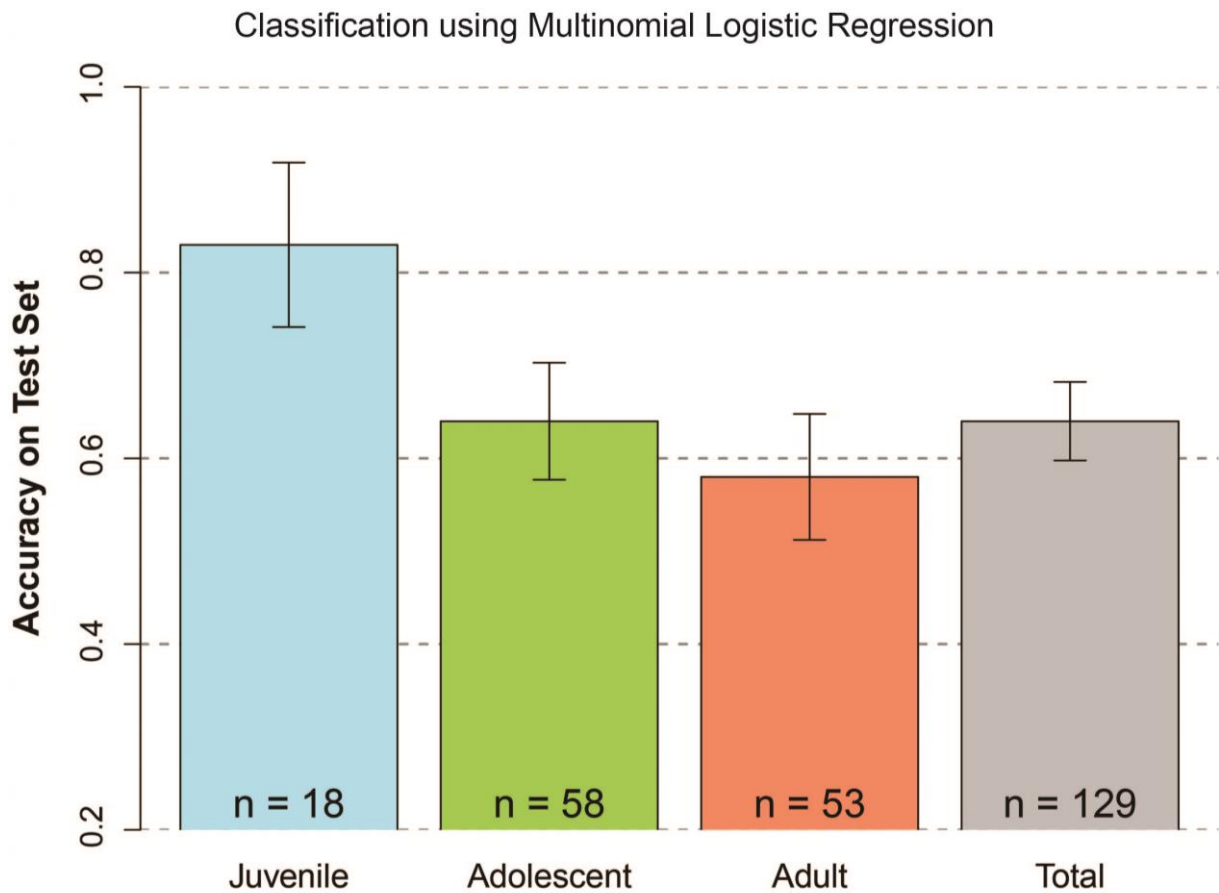
22
23 **Supplementary Figure S2: Quality control for zebrafish beta-cells used to develop**
24 **GERAS**

25 A flowchart showing the steps for determining sequencing quality. The following quality
26 control parameters were obtained for the entire dataset:

- 27 1. The median and median absolute deviation (MAD) for total reads
- 28 2. The median and MAD for % of mitochondrial reads
- 29 3. The median and MAD for % spike-ins
- 30 4. Number of detectable genes

31 Cells passed quality control if they belonged to median \pm 3*MAD bracket for 1-3 and
32 contained more than 1500 genes.

33 **Supplementary Figure S3**



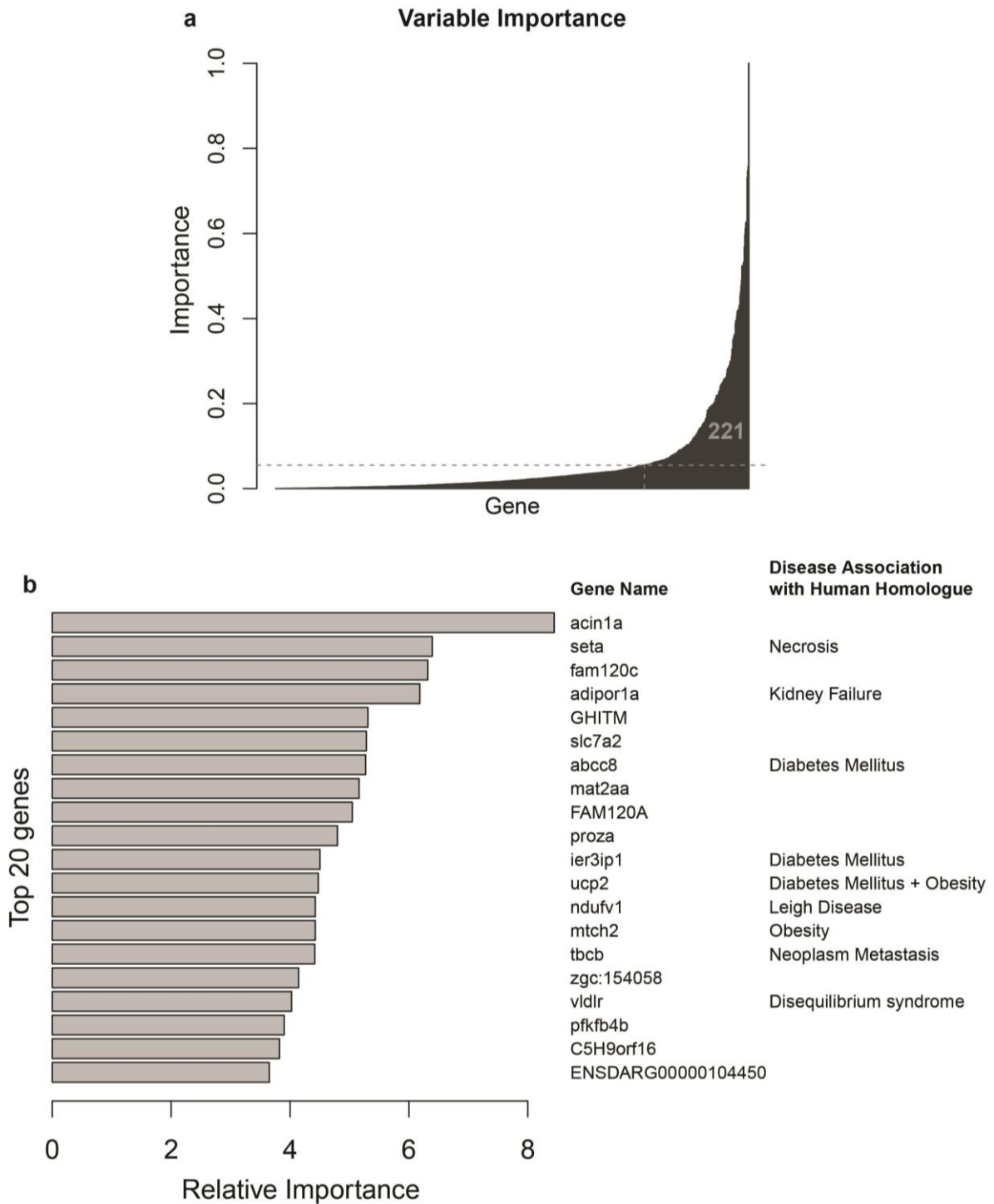
34

35 **Supplementary Figure S3: Classification of chronological stages using Multinomial**
36 **Logistic Regression**

37 Barplot showing the accuracy of a Multinomial Logistic Regression for classifying the age of
38 zebrafish beta-cells on the test set – the cells that were excluded from the training of the
39 logistic regression model. The classifications on the test display an overall accuracy of 64%.
40 Error bars indicate standard error. Multinomial Logistic Regression was carried out using the
41 ‘nnet’¹ package in R.

42

43 **Supplementary Figure S4**



44

45 **Supplementary Figure S4: Variable importance for zebrafish beta-cell GERAS**

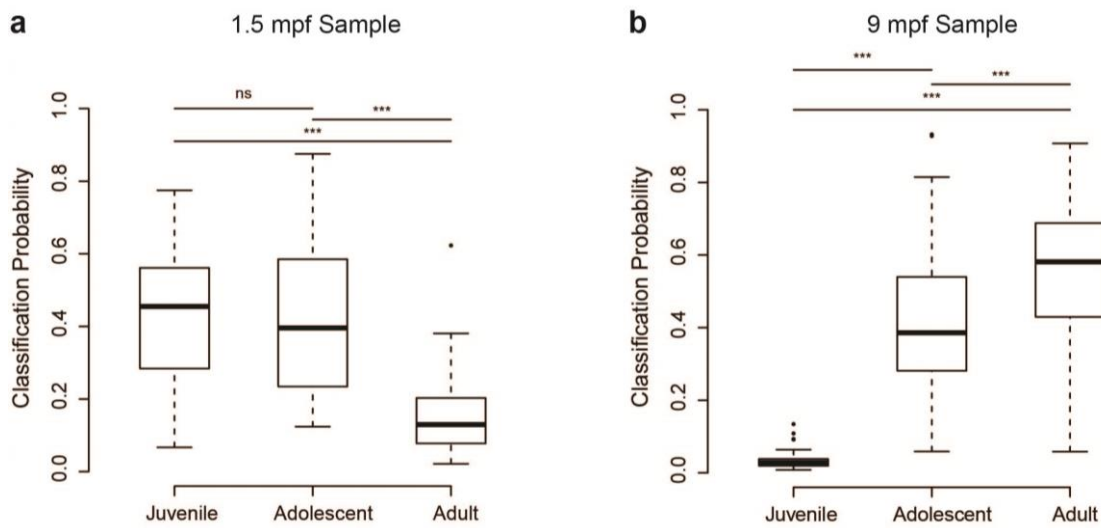
46 **(a)** Plot depicting the importance of each variable (gene) for the classification using zebrafish

47 beta-cell GERAS. The importance of each input gene is calculated using the strength

48 (weights) of the neural network connections². An input gene with stronger neural network
49 connections will be more important than another input gene with weaker neural network
50 connections. The Y-axis denotes variable importance, with 1 being most important and 0
51 being least important. On X-axis, all 1000 genes used as input to GERAS are depicted. Dotted
52 horizontal line depicts the mean of the variable importance. 221 genes (lying right of the
53 vertical dotted line) have importance higher than the mean.

54 **(b)** Barplot showing the relative importance of the top 20 genes. The X-axis denotes the
55 relative importance, and the Y-axis lists each gene individually. The names of the genes are
56 listed, along with the disease associated with their human homologue. Diseases association
57 were obtained from DisGeNET database³.

58 **Supplementary Figure S5**



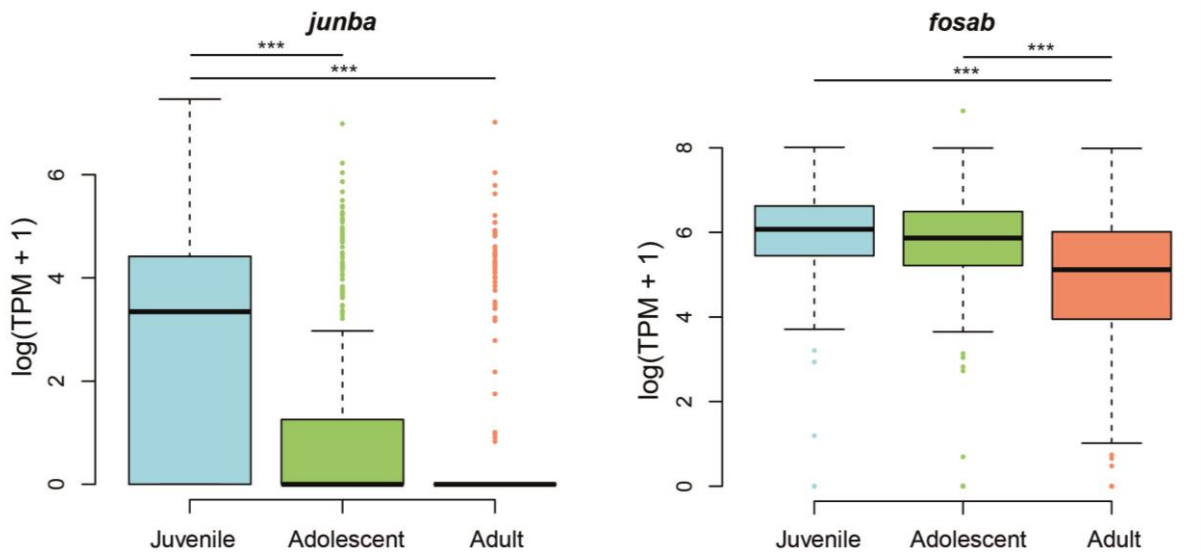
59

60 **Supplementary Figure S5: Classification probability for the ‘Interpolation’ samples**

61 **(a)** Boxplot depicting the classification probability for beta-cells collected from 1.5 mpf
62 animals. The probability for beta-cells from 1.5 mpf animals to be classified into the
63 ‘Juvenile’ stage (mean = 0.43) is statistically similar to the probability for the samples to be
64 classified into the ‘Adolescent’ stage (mean = 0.42). In contrast, the samples display a lower
65 probability to be classified into the ‘Adult’ stage (mean = 0.15). (ANOVA, p-value < 0.001;
66 Tukey’s test: ns, p-value > 0.05; *** p-value < 0.001).

67 **(b)** Boxplot depicting the classification probability for beta-cells collected from 9 mpf
68 animals. The samples display the highest probability to be classified into the ‘Adult’ stage
69 (mean = 0.56), followed by classification into the ‘Adolescent’ stage (mean = 0.41). The
70 samples display the lowest probability to be classified into the ‘Juvenile’ stage (mean = 0.03).
71 (ANOVA, p-value < 0.001; Tukey’s test: *** p-value < 0.001).

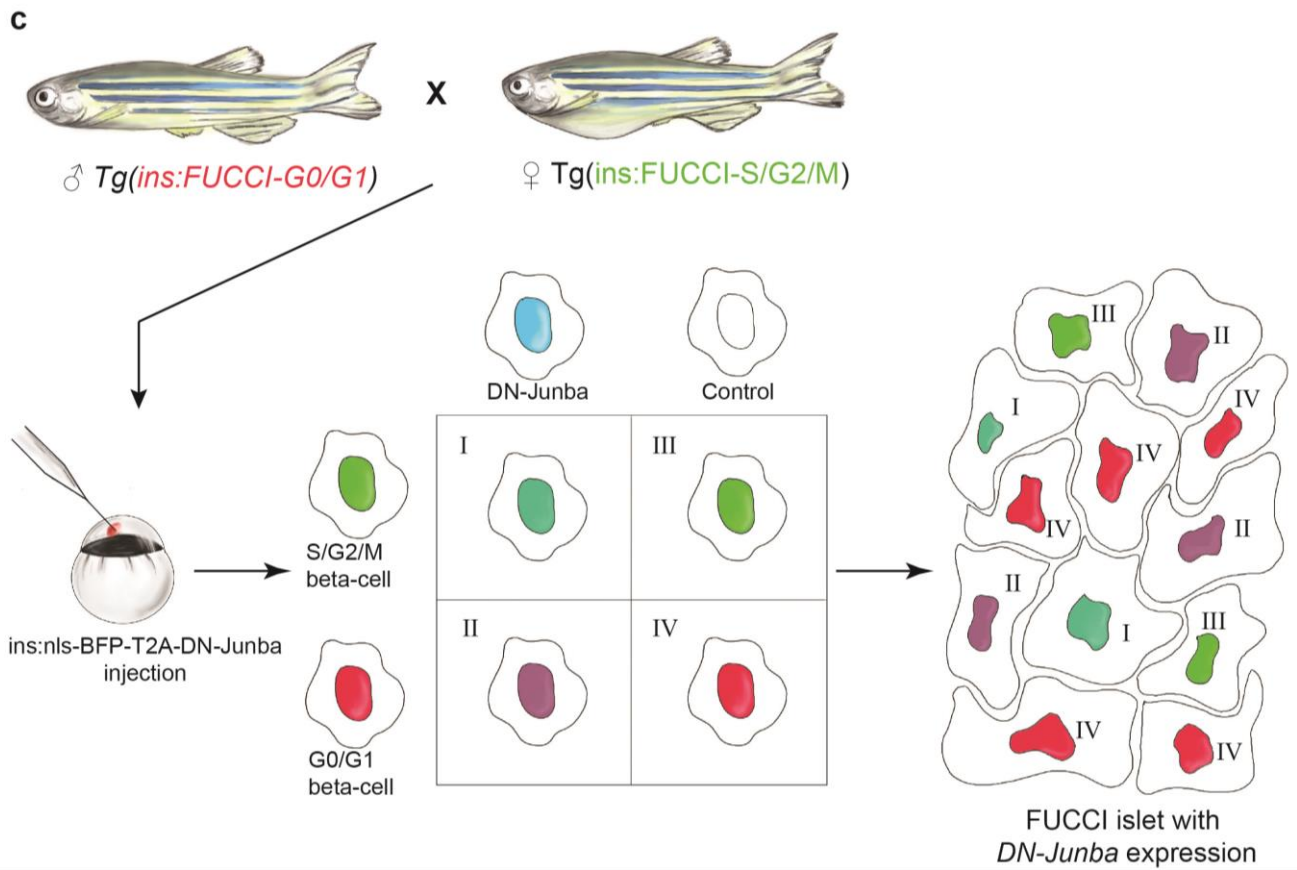
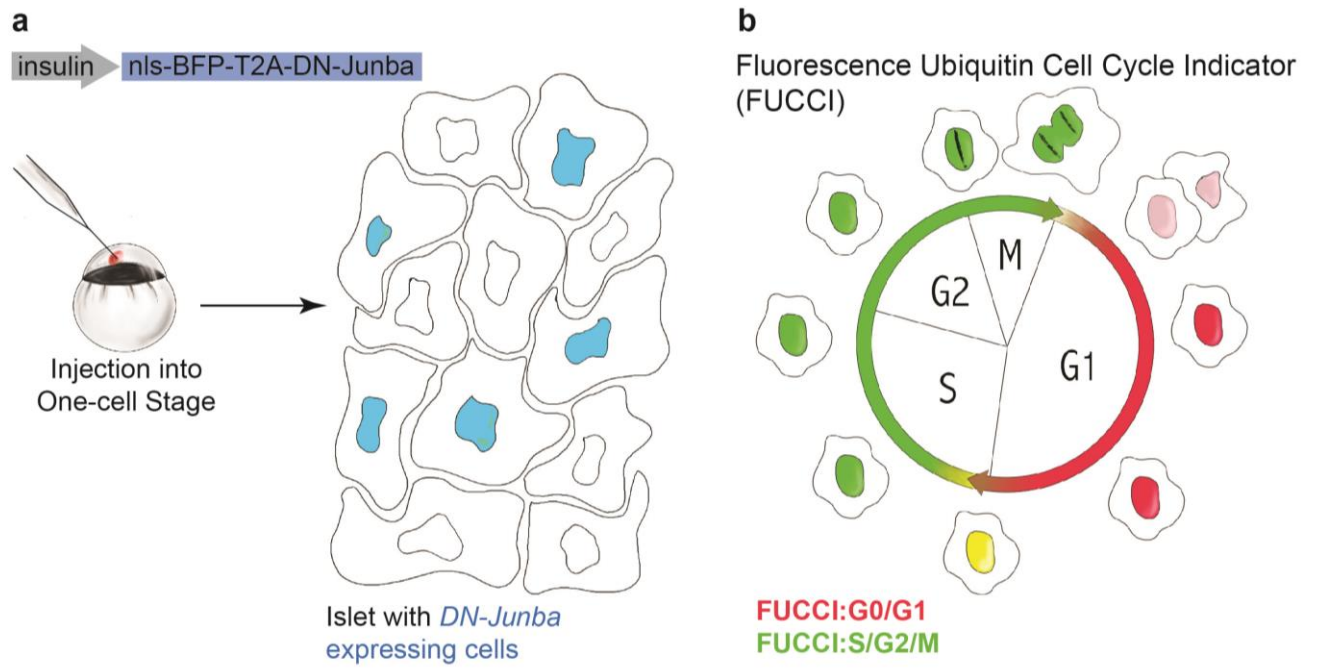
72 **Supplementary Figure S6**



73

74 **Supplementary Figure S6: Gene expression dynamics with age**

75 Tukey-style boxplots showing expression of *junba* (left) and *fosab* (right) in single beta-cells
76 during aging. Both genes show statistically significant down-regulation with age (t-test using
77 the ROTS package⁴, ***p-value < 0.001).



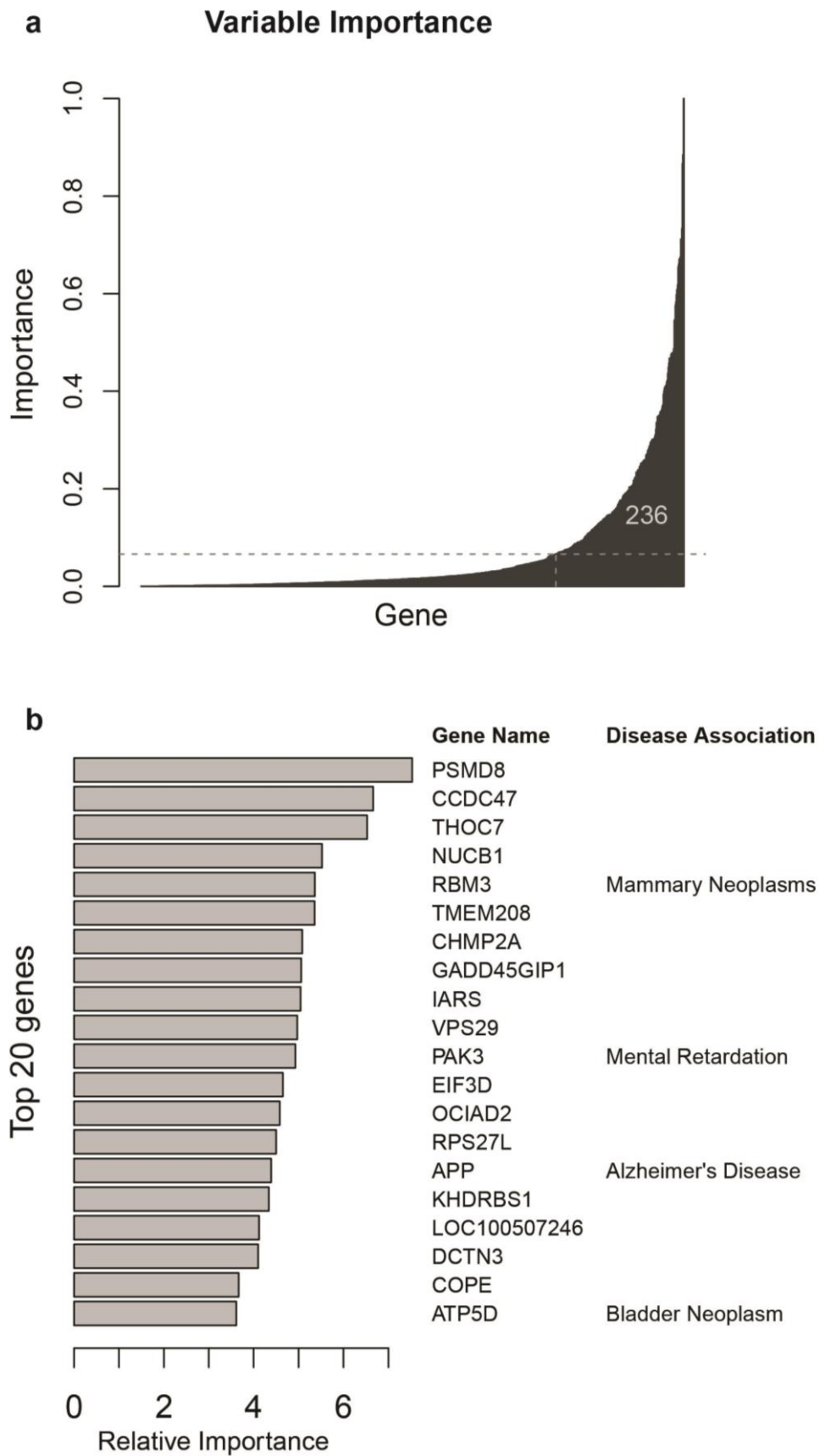
81 **Supplementary Figure S7: Setup of mosaic analysis for evaluating the impact of *DN-***
82 ***junba* on beta-cell proliferation.**

83 **(a)** Illustration depicting the generation of genetic mosaics. Zebrafish embryos are injected at
84 one-cell stage with a plasmid expressing the blue fluorescence protein tagged *DN-junba* from
85 the insulin promoter. The insulin promoter restricts expression to beta-cells. Random
86 integration of the genetic cassette leads to expression of *DN-junba* in a subset of beta-cells,
87 which are labeled in blue color.

88 **(b)** A schematic describing labeling of different cell-cycle states using the fluorescence
89 ubiquitination cell cycle indicator (FUCCI) system. FUCCI system includes two
90 components⁵. The FUCCI-G0/G1 fusion protein is degraded during S/G2/M phase, while
91 FUCCI-S/G2/M is spared. This leads to green fluorescence during S/G2/M phase. In contrast,
92 during G0/G1 phase, FUCCI-S/G2/M is degraded and FUCCI-G0/G1 is spared.

93 **(c)** Combining genetic mosaics with FUCCI system allows comparison of proliferation among
94 the *DN-junba*-expressing and control cells within the same islet. In this scenario, injection of
95 plasmid is performed in eggs collected from mating of transgenic animals containing the
96 individual FUCCI components. The injected animals grow to yield islets with *DN-junba*-
97 expressing and non-expressing cells. Proliferation is quantified based on the FUCCI-S/G2/M
98 and FUCCI-G0/G1 reporters.

99

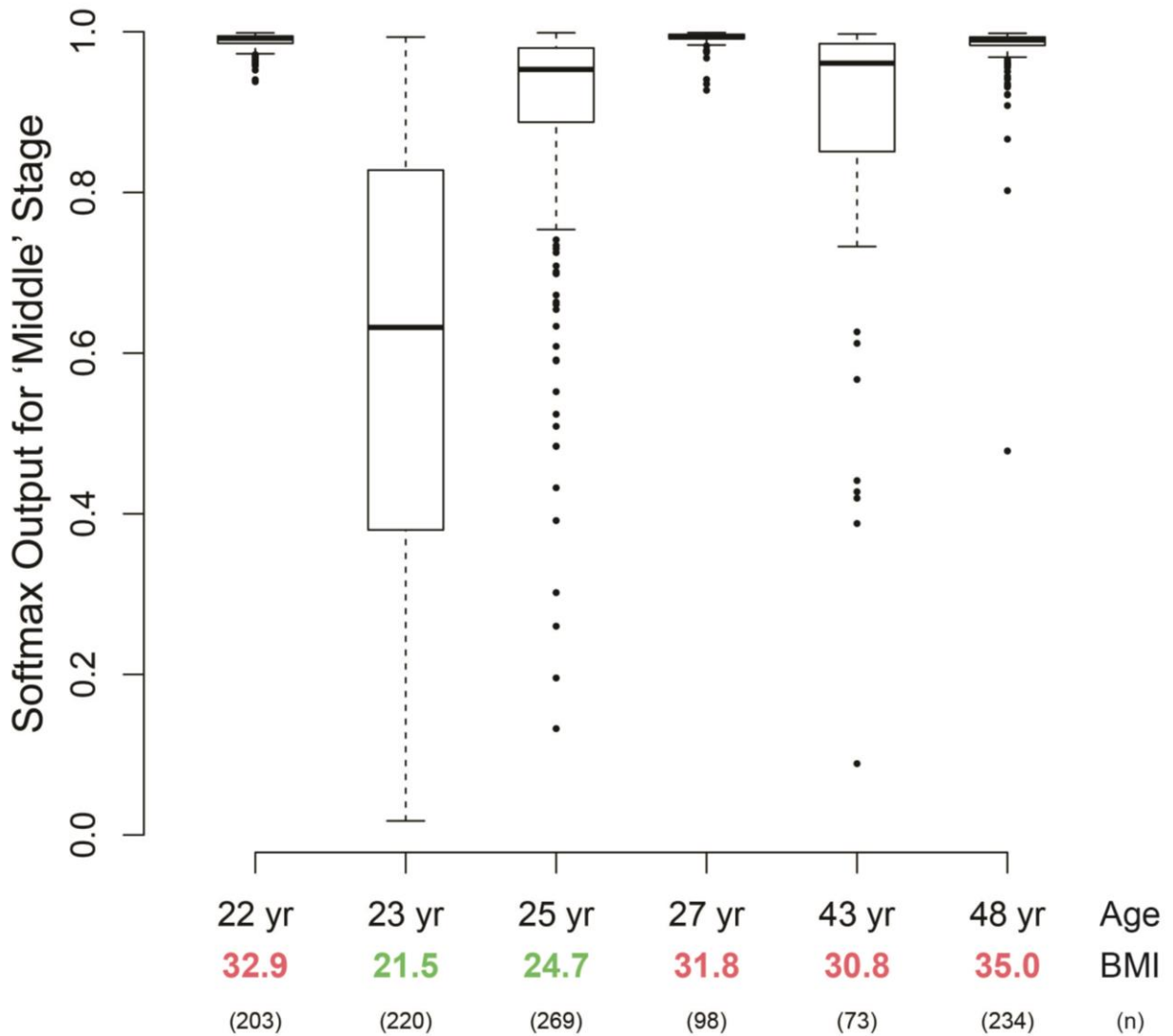


102 **Supplementary Figure S8: Variable importance for human pancreatic GERAS**

103 **(a)** Plot depicting the importance of each variable (gene) for the classification using human
104 pancreatic GERAS. The Y-axis depicts the importance of the variable from 0 (the lowest) to 1
105 (the highest). The X-axis shows the 1000 genes used as input to GERAS. The mean of the
106 variable importance is depicted by the dotted horizontal line; with 236 genes (lying right of
107 the vertical dotted line) having higher importance than the mean.

108 **(b)** Barplot showing the relative importance of the top 20 genes. Relative importance is
109 plotted on X-axis, and each gene is individually listed on the Y-axis. The names of the genes,
110 along with the disease associated with them is stated on the right. Diseases association were
111 obtained from DisGeNET database³.

Probability for Classification in 'Middle' (38 - 54 yr) Stage



113

114

115

116 **Supplementary Figure S9: Probability of cells from individuals ranging from 22 – 48**
117 **years to classify in the ‘Middle’ (38 – 54 years) stage**

118 Tukey-style boxplots showing the softmax output for the data from healthy individuals in
119 Segerstolpe et al.⁶ The softmax output for the ‘Middle’ stage of a single cell equals the
120 probability that the cell would classify in the ‘Middle’ stage. Individuals on the X-axis are
121 shown in ascending age. BMI for each individual is shown below the age and color coded
122 according to the BMI ranges indicated below. The BMI ranges are based on world health
123 organization (WHO) recommendations⁷. Numbers of cells from each individual are indicated
124 below the BMI values.

125

126 **Supplementary Table Legends**

127

128 **Table S1: Samples for development of GERAS for zebrafish beta-cells (.xls)**

129 A table listing the batches in which beta-cells were collected for the development of GERAS
130 for zebrafish beta-cells.

131

132 **Table S2: Variable Importance for zebrafish beta-cell GERAS (.xls)**

133 A table listing the 1000-input genes utilized by zebrafish beta-cell GERAS and their
134 importance towards classification.

135

136 **Table S3: Differential gene expression analysis between the beta-cells classified as
137 ‘Adult’ or ‘Adolescent’ from zebrafish fed three-times-a-day (.xls)**

138 A table listing the differences in gene expression between beta-cells classified as ‘Adult’ vs.
139 beta-cells classified as ‘Adolescent’ from the cells collected from zebrafish fed three-times-a-
140 day. The table lists all the genes in descending order of false-discovery rate (FDR). Genes that
141 show differential gene expression (FDR < 0.05) are italicized.

142

143 **Table S4: Differential gene expression analysis between the transcriptome of beta-cells
144 collected zebrafish on intermittent feeding vs. the transcriptome of beta-cells collected
145 from zebrafish fed three-times-a-day (.xls)**

146 A table listing the differences in gene expression between beta-cells collected from zebrafish
147 on intermittent feeding vs. three-times-a-day fed zebrafish. The table lists all the genes in
148 descending order of false-discovery rate (FDR). Genes that show differential gene expression
149 (FDR < 0.05) are italicized.

150

151 **Table S5: Variable Importance for Human pancreatic GERAS (.xls)**

152 A table listing the 1000-input genes utilized by human pancreatic GERAS and their
153 importance towards classification.

154

155 **Supplementary Methods**

156 **Single cell isolation of zebrafish beta-cells**

157 Primary islets from *Tg(ins:BB1.0L; cryaa:RFP)* zebrafish were dissociated into single
158 cells and sorted using FACS-Aria II (BD Bioscience). Islets were dissociated into single cells
159 by incubation in TrypLE (ThermoFisher, 12563029) with 0.1% Pluronic F-68 (ThermoFisher,
160 24040032) at 37 °C in a benchtop shaker set at 450 rpm for 30 min. Following dissociation,
161 TrypLE was inactivated with 10% FBS, and the cells pelleted by centrifugation at 500g for 10
162 min at 4 °C. The supernatant was carefully discarded and the pellet re-suspended in 500 uL of
163 HBSS (without Ca, Mg) + 0.1% Pluronic F-68. To remove debris, the solution was passed
164 over a 30 µm cell filter (Miltenyi Biotec, 130-041-407). To remove dead cells, calcein violet
165 (ThermoFisher, C34858) was added at a final concentration of 1 µM and the cell suspension
166 incubated at room temperature for 20 minutes. The single cell preparation was sorted with the
167 appropriate gate for identification of beta-cells (RFP+ and calcein+) (Supplementary Fig. S1).
168 FACS was performed through 100 µm nozzle with index sorting.

169 Beta-cells were collected from seven ages of zebrafish: 1 mpf, 3 mpf, 4 mpf, 6 mpf, 10
170 mpf, 12 mpf and 14 mpf. For classification, the seven ages were divided into three
171 chronological stages: 'Juvenile' (1 mpf), 'Adolescent' (3, 4 and 6 mpf) and 'Adult' (10, 12
172 and 14 mpf). The collection of the beta-cells was carried out in four batches (Supplementary
173 Table S1), with each batch representing a different collection date. In Supplementary Table
174 S1, the four batches (collection dates) are labeled as 'A', 'B', 'C' and 'D' for simplification. It
175 is important to note that each batch (except 'D') contained samples from more than one
176 chronological stage and conversely each stage (except 'Juvenile') was represented in more
177 than one batch.

178 **Single cell mRNA sequencing of zebrafish beta-cells from 96-well plates**

179 Cells were sorted into a 96-well plate containing 2 µl of nuclease free water with 0.2%
180 Triton-X 100 and 4 U murine RNase Inhibitor (NEB), spun down and frozen at -80°C. After
181 thawing the samples, 2 µl of a primer mix was added (5 mM dNTP (Invitrogen), 0.5 µM dT-
182 primer*, 4 U RNase Inhibitor (NEB)). RNA was denatured for 3 minutes at 72°C and the
183 reverse transcription was performed at 42°C for 90 min after filling up to 10 µl with RT
184 buffer mix for a final concentration of 1x superscript II buffer (Invitrogen), 1 M betaine, 5
185 mM DTT, 6 mM MgCl₂, 1 µM TSO-primer*, 9 U RNase Inhibitor and 90 U Superscript II.
186 After synthesis, the reverse transcriptase was inactivated at 70°C for 15 min. The cDNA was
187 amplified using Kapa HiFi HotStart Readymix (Peqlab) at a final 1x concentration and 0.1
188 µM UP primer under following cycling conditions: initial denaturation at 98°C for 3 min, 22
189 cycles [98°C 20 sec, 67°C 15 sec, 72°C 6 min] and final elongation at 72°C for 5 min. The
190 amplified cDNA was purified using 1x volume of hydrophobic Sera-Mag SpeedBeads (GE
191 Healthcare) and DNA was eluted in 12 µl nuclease free water. The concentration of the
192 samples was measured with a Tecan plate reader Infinite 200 pro in 384 well black flat
193 bottom low volume plates (Corning) using AccuBlue Broad range chemistry (Biotium).

194 For library preparation, 700 pg cDNA in 2 µl was mixed with 0.5 µl tagmentation
195 enzyme and 2.5 µl Tagment DNA Buffer (Nextera DNA Library Preparation Kit; Illumina)
196 and tagmented at 55°C for 5 min. Subsequently, Illumina indices were added during PCR
197 (72°C 3 min, 98°C 30 sec, 12 cycles [98°C 10 sec, 63°C 20 sec, 72°C 1 min], 72°C 5 min)
198 with 1x concentrated KAPA Hifi HotStart Ready Mix and 0.7 µM dual indexing primers.
199 After PCR, libraries were quantified with AccuBlue Broad range chemistry, equimolarly
200 pooled and purified twice with 1x volume Sera-Mag SpeedBeads. This was followed by
201 Illumina sequencing on a Nextseq500 aiming at an average sequencing depth of 0.5 million
202 reads per cell.

203

204 *dT primer: Aminolinker-AAGCAGTGGTATCAACGCAGAGTCGAC T(30) VN

205 *TSO primer: AAGCAGTGGTATCAACGCAGAGTACATggg

206 *UP primer: AAGCAGTGGTATCAACGCAGAGT

207 The C1™ Single-Cell mRNA Seq 10-17 µm IFC (© Fluidigm Corporation, CA, USA) was
208 used to perform mRNA sequencing on single cells. In general, the protocol (PN 100-7168 L1)
209 suggested by the manufacturer was followed, with some modifications. 1200 cells in PBS
210 were directly sorted by FACS into the inlet, mixed 3:2 with suspension reagent, resulting in a
211 final volume of 6 µl. Cells were loaded with the mRNAseq: Cell load protocol, without
212 staining on the IFC. For RT and amplification, the mRNA Seq: RT & Amp script was run
213 with the following cycling parameters: 1x 98°C 1 min, 5x (95°C 20-45 sec, 59-49°C with
214 0.3°C increment/cycle 4 min, 68°C 6 min) 9x (95°C 20-45 sec, 65-49°C with 0.3°C
215 increment/cycle 30 sec, 68°C 6 min) 7x (95°C 30-45 sec, 65-49°C with 0.3°C increment/cycle
216 30 sec, 68°C 7 min) and 72°C 10 min using SMART-Seq v4 Ultra Low Input RNA Kit for
217 Sequencing (Takara BIO USA, INC.). For library preparation, 2 µl cDNA were mixed with
218 0.5 µl tagmentation enzyme and 2.5 µl Tagment DNA Buffer (Nextera DNA Library
219 Preparation Kit; Illumina) and tagmented at 55°C for 5 min. Illumina indices were added by
220 PCR with the following cycling conditions: 1x (72°C 3 min, 98°C 30 sec), 12 x (98°C 10 sec,
221 63°C 20 sec, 72°C 1 min), 1x (72°C 5 min), using KAPA Hifi HotStart Ready Mix and 0.7
222 µM final dual indexing primers. Libraries were quantified, equimolarly pooled and purified
223 twice with 1x volume Sera-Mag SpeedBeads. Illumina sequencing (75bp SE) was done on a
224 Nextseq500 aiming to achieve an average sequencing depth of 0.5 million reads per cell.

225 **Mapping of read counts and quality control**

226 Raw reads in fastq format were trimmed using trim-galore with default parameters to
227 remove adapter sequences. Trimmed reads were aligned to the zebrafish genome, GRCz10,
228 using HISAT2⁸ with default parameters. htseq-count⁹ was used to assign reads to exons thus
229 eventually getting counts per gene. Using cells that were utilized for developing zebrafish
230 GERAS (see next section), the following quality control parameters were obtained
231 (Supplementary Fig. S2):

- 232 1. The median and median absolute deviation (MAD) for total reads
- 233 2. The median and MAD for % of mitochondrial reads
- 234 3. The median and MAD for % spike-ins
- 235 4. Number of detectable genes

236 Cells passed quality control if they belonged to median \pm 3*MAD bracket for 1-3 and
237 contained more than 1500 genes. Read counts for all cells that passed quality control are
238 available from GEO under accession number GSE109881.

239 **Development of a Multinomial Logistic Regression Model for zebrafish beta-cells**

240 For development of multinomial logistic regression for zebrafish beta-cells, TPM
241 normalized counts were used from seven ages of zebrafish distributed into three chronological
242 stages: 1 mpf ('Juvenile'); 3 mpf, 4 mpf and 6 mpf ('Adolescent'); 10 mpf, 12 mpf and 14
243 mpf ('Adult'). The entire dataset containing 508 beta-cells were randomly divided into 80%-
244 20% train-test set. Multinomial Logistic Regression model was developed using the 'nnet'¹
245 package in R using the top most variable genes (Supplementary Table S2). With 1000 and
246 500 top-variable genes, the variance-covariance matrix could not be calculated. Variance-
247 covariance matrix could be calculated for an input of 250 genes. Thus, we developed a model
248 using 250-top variable genes using *model* \leftarrow *multinom* (*stage* ~ *gene*, *data* =

249 *ExpressionData*). The code for developing the Multinomial Logistic Regression Model is
250 uploaded as ZF_MultipleLogisticRegression.R on github ¹⁰.

251 The trained model was used to classify the chronological age of the test set.
252 Accuracy was calculated as the proportion of cells for which the classification matched the
253 chronological age. By considering each classification as a binomial distribution (a ‘Juvenile’
254 cell can be classified as ‘Juvenile’ or ‘Not Juvenile’), the standard error was calculated using
255 the following formula:

$$\text{Standard error} = \sqrt{\frac{\text{accuracy} * (1 - \text{accuracy})}{n}}$$

256 where *n* is the number of cells tested.

257 **Construction of the *ins:nls-BFP-T2A-DN-junba*; *cryaa:RFP* plasmid**

258 To generate *ins: nls-BFP-T2A-DN-junba;cryaa:RFP*, a vector was created by
259 inserting multiple cloning sites (MCS) downstream of the insulin promoter to yield *ins:MCS*;
260 *cryaa:RFP*. To do so, the plasmid *ins:mAG-zGeminin;cryaa:RFP* was digested with
261 EcoRI/PacI and ligated with dsDNA generated by annealing two primers harboring the sites
262 EcoRV, NheI, NsiI, Sall and flanked by EcoRI/PacI overhangs. The plasmid pUC-Kan
263 consisting of the DN-junba (*junba*¹⁵⁷⁻³²⁵, consisting of only the DNA binding domain¹¹) fused
264 to *nls-BFP* via T2A sequence flanked by EcoRI/PacI sites was synthesized from GenScript.
265 *ins:MCS;cryaa:RFP* and the plasmid *pUC-nls-BFP-T2A-DN-junba* were subsequently
266 digested with EcoRI/PacI to yield compatible fragments, which were ligated together to yield
267 the final construct. The entire construct was flanked with I-SceI sites to facilitate genomic
268 insertion.

269 **Analysis of proliferation using mosaic expression of *DN-junba***

270 To identify proliferating beta-cells, the zebrafish beta-cell specific FUCCI system¹²
271 was used by crossing *Tg(ins:FUCCI-G1)* with *Tg(ins:FUCCI-S/G2/M)*. Embryos obtained
272 from the mating were injected with *ins:nls-BFP-T2A-DN-junba;cryaa:RFP* plasmid, along
273 with I-SceI, to facilitate mosaic integration into the genome. At 30 dpf, animals were
274 euthanized in Tricaine and dissected to isolate the islets. The isolated islets were fixed in 4%
275 paraformaldehyde (PFA) for 48 hours at 4°C, washed multiple times in PBS and mounted on
276 slides for confocal microscopy. Confocal images were used for cell-counting. All the
277 *Tg(ins:FUCCI-S/G2/M)*-positive cells (green fluorescence only) were counted manually
278 within the BFP-positive and BFP-negative clones. Using Imaris (Bitplane), the total number
279 of BFP-positive and beta-cells were calculated in the entire islet. For this, the “spots” function
280 was used after thresholding. For calculating percentages (%), the following calculations were
281 used:

$$\text{Total BFP-negative cells} = \text{Total beta-cells} - \text{Total BFP-positive cells}$$

% BFP-positive proliferating cells

$$= \frac{\text{ins:FUCCI-S/G2/M-positive and BFP-positive cells}}{\text{Total BFP-positive cells}} * 100$$

% BFP-negative proliferating cells

$$= \frac{\text{ins:FUCCI-S/G2/M-positive and BFP-negative cells}}{\text{Total BFP-negative cells}} * 100$$

282 **Calculating variable importance for GERAS**

283 Variable importance was calculated as outlined in Gedeon et al.². The code for
284 carrying out the calculation is shared as source/variableImportance.R on github¹⁰. The code
285 uses the weights of the trained neural network to calculate the importance of each variable
286 (input) used for classification. The output is scaled to 0 (least important) and 1 (most

287 important). This was used to identify the importance of each gene used in zebrafish and
288 human GERAS. The results were sorted in descending order for plotting. Additionally, the top
289 20 most important genes were obtained from the sorted list, and their relative importance
290 calculated using the formula,

$$Relative\ Importance_g = \frac{Importance_g}{\sum_g Importance}$$

291 where g denotes an individual gene among the top 20. The disease association for each gene
292 was obtained from DisGeNET database ³. From the database, an association with a score of
293 greater than or equal to 0.2 was reported.

294 **Shiny implementation of GERAS classifier**

295 To enable easy access to classifications using GERAS, a Shiny app was developed.
296 The app is freely available on Github ¹⁰. The app provides a graphic-user interface (GUI) for
297 users to make chronological age classifications using a pre-trained GERAS model. The users
298 can upload normalized counts, verify the uploaded data, and obtain classifications in a
299 downloadable comma-separated (csv) file.

300

301

302

303 **Supplementary References:**

304

305 1. Venables, W. N. & Ripley, B. D. *Modern Applied Statistics with S*. (Springer, 2002).

306 2. Gedeon, T. D. Data mining of inputs: analysing magnitude and functional measures.
307 *Int. J. Neural Syst.* **8**, 209–18 (1997).

308 3. Piñero, J. *et al.* DisGeNET: a comprehensive platform integrating information on
309 human disease-associated genes and variants. *Nucleic Acids Res.* **45**, D833–D839
310 (2017).

311 4. Suomi, T., Seyednasrollah, F., Jaakkola, M. K., Faux, T. & Elo, L. L. ROTS: An R
312 package for reproducibility-optimized statistical testing. *PLOS Comput. Biol.* **13**,
313 e1005562 (2017).

314 5. Sakaue-Sawano, A. *et al.* Visualizing spatiotemporal dynamics of multicellular cell-
315 cycle progression. *Cell* **132**, 487–98 (2008).

316 6. Segerstolpe, Å. *et al.* Single-Cell Transcriptome Profiling of Human Pancreatic Islets
317 in Health and Type 2 Diabetes. *Cell Metab.* 593–607 (2016).
318 doi:10.1016/j.cmet.2016.08.020

319 7. World Health Organization. Global database on body mass index. (2011).

320 8. Kim, D., Langmead, B. & Salzberg, S. L. HISAT: a fast spliced aligner with low
321 memory requirements. *Nat. Methods* **12**, 357–360 (2015).

322 9. Anders, S., Pyl, P. T. & Huber, W. HTSeq--a Python framework to work with high-
323 throughput sequencing data. *Bioinformatics* **31**, 166–169 (2015).

324 10. Singh, S. P. GERAS (GENetic Referene for Age of Single-cell).

325 <https://github.com/sumeetpalsingh/GERAS2017> (2017).

326 11. Castellazzi, M. *et al.* Overexpression of c-jun, junB, or junD affects cell growth
327 differently. *Proc. Natl. Acad. Sci. U. S. A.* **88**, 8890–4 (1991).

328 12. Ninov, N. *et al.* Metabolic regulation of cellular plasticity in the pancreas. *Curr. Biol.*
329 **23**, 1242–1250 (2013).

330